World Applied Sciences Journal 30 (3): 335-340, 2014
ISSN 1818-4952

DOI: 10.5829/idosi.wasj.2014.30.03.2643

Characterizations of Martensite in Fe-30%Ni-3%Pd Alloy

Yasin Göktürk Yildiz and Gökçen Yildiz

Department of Physics, Science and Arts Faculty, Kirikkale University, Kirikkale, 71450, Turkey

Abstract: Morphological, magnetic and thermal characteristics of thermally induced martensite in Fe–30% Ni–3% Pd (wt.%) alloy has been studied by scanning electron microscopy (SEM), transmission electron microscopy (TEM), differential scanning calorimeter (DSC), X-ray diffraction (XRD) method and Mössbauer spectroscopy. Kinetics of the transformation was found to be as athermal. Plate martensite morphology was observed during microscope observations. SEM and TEM observations and x-ray method revealed α′ (bcc) martensite formation with twinning. The crystallographic orientation relationship between the austenite and martensite exhibited a $(1\bar{1}0)\alpha' // (\bar{1}11)_{\gamma}\ [111]\alpha' // [110]_{\gamma}$ K-S type orientation relationship. The mean value of the lattice parameter of the austenite and martensite phase calculated as 3.5704 ε and 2.8614 ε respectively. In addition, the magnetic properties of both the austenite and martensite phases were determined by the Mössbauer spectroscopy. The Mössbauer spectra showed a paramagnetic character for the austenite phase and a ferromagnetic (or antiferromagnetic) character for the martensite phase. Also, Mössbauer studies shows that the value of hyperfine field increases with an addition of Pd element.

Key words: FeNiPd Alloy · Martensitic Transformations · Electron Microscopy · X-Ray Diffraction · Athermal Kinetics · Mössbauer Spectroscopy

INTRODUCTION

The martensitic transformation is one of typical first-order structural phase transitions without atom diffusion and has been widely studied to determine its characteristics from physical, metallographical and crystallographic view points [1]. It is well known that martensitic transformations are influenced by external fields, such as thermall effects, hydrostatic pressure and uniaxial stress. Therefore, studies on the effects of these external fields are important to understand the essential problems of the martensitic transformation such as thermodynamics, kinetics and the origin of the transformation [2- 5].

A significant property of martensitic phase transformations in Fe-Ni alloys, the morphology of martensite dependent on Ni percentage [4]. Furthermore, addition of Mn, Co, C, etc. as a third alloying element to binary Fe-Ni alloys changes some properties of martensitic transformations such as kinetics of the transformation and morphology of the martensite [5-8]. Previous results have been reported on lath, butterfly, lenticular, plate and thin-plate morphologies for martensitic transformations in different ferrous alloys [9-12].

Two different types of martensitic transformation kinetics, named athermal and isothermal kinetics. Although the athermal kinetics depends only on temperature, isothermal kinetics depends both on time and temperature during transformations [13]. Mostly seen athermal kinetics occurs at a well defined M_s temperature. Besides the time of formation of a single plate of martensite in an iron-nickel alloy to be approximately 1.10^{-7} s [14].

From a magnetic viewpoint of Fe-based alloys, another significant property of the martensite is its distinguished magnetic character from austenite. In spite of the paramagnetic nature of the austenitic parent phase in these alloys, martensitic product phase can show either ferromagnetic or antiferromagnetic behaviours [15]. It is known that the local coupling contains two contributions. One is the local or inner s-electrons which

Corresponding Author: Yasin Göktürk Yildiz, Science and Arts Faculty, Department of Physics, Kirikkale University, Kirikkale, 71450, Turkey. Tel: +903183574242.

are polarized by the unpaired 3d-electrons-the origin of the local atomic magnetic moment. The other is the contribution from the itinerant 4s-conduction electrons which are also polarized by the local unpaired 3d-electrons. The increased magnetic field is related to an increased localization of the 3d electrons. Furthermore, previous Mössbauer studies have found that the Hyperfine magnetic field is 32 T for Fe-%30 Ni alloys [16]. Also Pd atoms cause a net increase in the magnetic moments at Fe sites [17] and the increase of ^{57}Fe Bhf with increasing Pd concentration [18].

Although many studies are present for thermally induced martensite in various Fe-Ni-X alloys, no work has reported for the Fe-30% Ni-3%Pd alloy. Therefore, the present study was to examine, morphology and martensite kinetics of thermally induced martensite in Fe-30 % Ni-3 % Pd alloy by TEM, SEM, DSC, X-Ray diffraction method and Mössbauer spectroscopy.

Experimentals: The alloy employed in the present study was Fe-30% Ni-3%Pd (wt.%) which was prepared by vacuum induction melting under an argon atmosphere from pure (%99.9) alloying elements. This alloy was cylindrical bars (1cm diameter and 10cm long). Bulk samples were homogenized at 1200°C in quartz tube for 6 h and then quenched in water at room temperature. These samples then mechanically thinned for SEM observations. The surface of the samples were mechanically polished and used chemical solution which contains 90 ml H_2O_2, 15 ml H_2O and 5 ml HF for clarifying samples surfaces. Surfaces of samples were carried out using a JEOL JSM 5600 type scanning electron microscope with 20 kV operating voltage. New thin foil samples (~50 µm) were prepared for transmission electron microscopy from the thermal-treated samples. These TEM specimens then were electropolished at room temperature using a twin-jet polishing technique with a solution of 150 ml 2-butoxy ethenol, 5 0 ml of perchloric acid and 300 ml methenol. The TEM observations were performed by a JEOL 3010 type TEM with 300 kV operating voltage. In order to determine M_s, A_s and A_f temperatures of transformation in Fe-%30 Ni-%3 Pd alloy, homogenized samples of this alloy were prepared in the shape of 1 mm diameter discs and encapsulated in aluminum pans. DSC samples of this alloy were performed by using a Perkin-Elmer Sapphire model thermal analyser and taken at a cooling rate of 5°C/min between 20°C and -150°C. The Mössbauer spectroscopy was carried out at room temperature by using 50m Ci ^{57}Co source diffused in Rh and a Norrmos-90 computer programme was used to determine the parameters and relative volume fractions of the product phase.

RESULTS AND DISCUSSION

Fig. 1a shows the secondary electron image of SEM micrograph of the austenite phase of Fe-30% Ni-3%Pd alloy with its typical austenite grain boundaries and average size of grains as found approximately 250 µm. Fig. 1b shows a SEM micrograph of this sample after the 5 s liquid nitrogen (-196 °C) immersion. This thermal stimulation caused martensite plates formation in Fig. 1b.

Troiano and Greninger [19] considered kinetics to be as important as crystallography in defining the characteristics of martensitic reactions [20]. In addition theoretical considerations of the martensitic transformations don't lead to any separation between nucleation during athermal and isothermal processes. Each theory attempted within its own limits to explain the athermality and isothermality of the reaction [21].

Transformation temperatures (M_s, A_s and A_f) were determined by differantial scannig calorimetry (DSC). From the DSC results, austenite start temperature (A_s) and austenite finish temperature (A_f) found as 380°C and 450°C respectively (Fig 2a). Besides martensite start temperature (M_s) found as -26°C (Fig 2b).

Some evidences such as new nucleation sites or growth of exiested martensite crystals achived by further isothermal martensitic transformations are well descriptioned by Kajiwara[13]. Although sample of the Fe-30%Ni-3%Pd alloy were kept at -196 °C for 10 min, 10 h and 10 days, these isothermal holding times didn't couse the formation of martensite crystals. This application suggest that the martensite kinetics displayed athermal type. Kaufman and Cohen [22] investigated the martensite start temperature (M_s) and the austenite start temperature (A_s) in the iron-nickel system have been determined between 9.5 and 33.2 atomic pct nickel. According to them, the $\gamma \rightarrow \alpha'$ transformation displays the burst phenomenon in alloys containing more than 28.00 % at nickel (%wt 29.08) and martensite start temperature for Fe-30.43%Ni alloy found as -30°C. Similar results of martensite start temperature of Fe-Ni binary alloys which contains nearly 30%Ni reported by some resarchers too. Their results given at Table 1.

The important point of this results, martensite start temperature is relatively insensitive to heating and cooling rate and heat treatments. As a remarkable result of

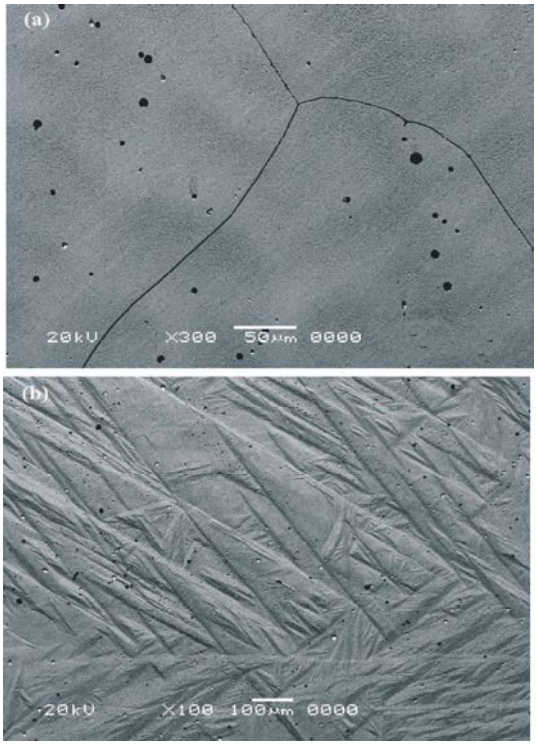

Fig. 1: SEM micrographs showing the microstructure of Fe-30%Ni-3%Pd alloy: (a) Austenite phase which have typical grain boundaries, (b) Surface relief of martensite plates formed on immersing in liquid nitrogen.

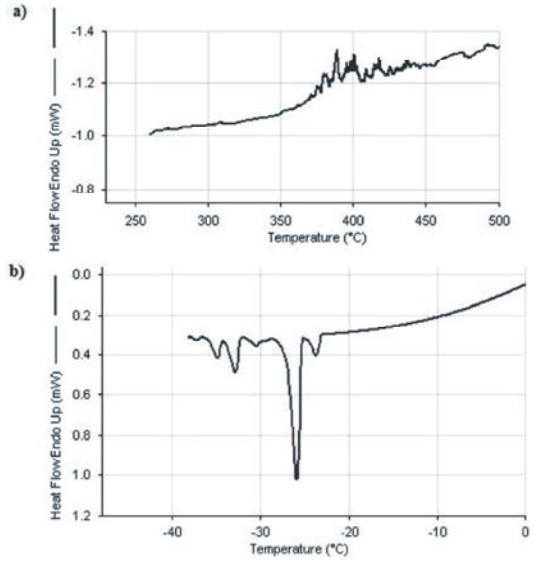

Fig. 2: DSC curves showing the transformation temperatures of alloy (a) A_s and A_f temperatures of thermally induced martensite in Fe-30% Ni-3%Pd alloy (b) M_s temperature of thermally induced martensite in Fe-30%Ni-3%Pd alloy

Table 1: M_S temperatures of the alloys used in the present and previous study

Sample (wt.%)		Ms(°C)
Fe-30%Ni-3%Pd (present study)		- 26
Fe-30.43%Ni	[22]	- 30
Fe-29.60%Ni	[23]	-39
Fe-31.00%Ni	[24]	-50

this study, M_s temperature did not show a major deviation with addition of 3% Pd to Fe-30%Ni binary alloy. On the other hand, previous results have been reported that, addition of Cr, Si and Mo as a third alloying element to binary Fe-Ni alloys, the M_s temperatures of thermally induced martensites were determined as -138°C for Fe-29.40% Ni-2% Cr alloy [12], -83°C for Fe-30% Ni-0.8% Mo alloy [15] and -180°C for Fe-28% Ni-7.5% Si alloy [25]. According to the present study, compared with the other elements (Cr, Si, Mo) the element of Pd increases the temperature of M_s.

A general mechanism of martensitic nucleation was olso given by Olson and Cohen [21]. The mechanism is consisted with the hetorogeneous nature of martensitic nucleation, the transformation crystallography and the basic athermal character of martensitic transformations. According to this mechanism, the nucleation process can be treated as a sequence of steps.

The first nucleation step consists of faulting on the closest packed planes of the parent phase, the fault displacement being derived from an existing defect and the subsequent steps in nucleation process take place in such a way as to leave the fault plane unrotated [26]. Besides martensitic transformations nucleation starts at dislocations [1]. Fig. 3a shows TEM micrograph of a typical dislocation network in Fe-30% Ni-3% Pd alloy. It is well known that each morphology is different in crystallography and substructure for ferrous alloys. The morphology of martensite depended on M_s temperature, austenite stacking fault energy, driving force associated with the transformation, the strength of martensite and austenite, critical resolved shear stres for slip and twinning in martensite [10].

Fig. 3b shows thermal induced martensite plates in Fe-30%Ni-3%Pd alloy. Besides the stacking faults appear obviously in austenite phase. They create embryos for the α' martensite formation. The orientation relationship between austenite and martensite is obtained as $(1\bar{1}0)\alpha' // (\bar{1}11)_\gamma\ [111]\alpha' // [110]_\gamma$ Kurdjumov-Sachs (K-S) type and the habit plane is determined as very close to $[252]_\gamma$ plane of the austenite. These crystallographic results were found in aggreement with the earlier reports [27,28].

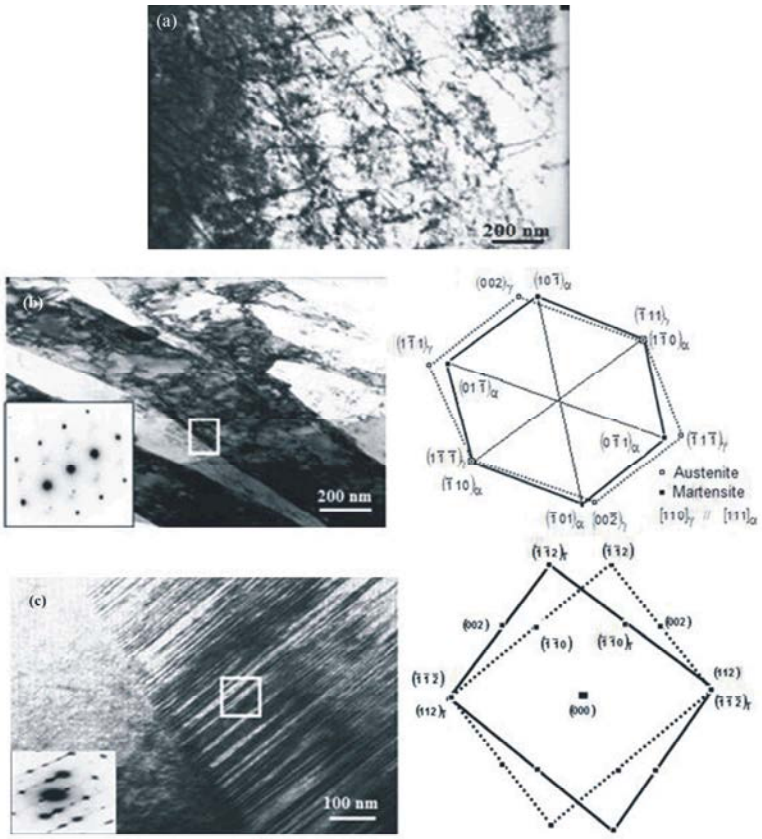

Fig. 3: TEM images of Fe-%30Ni-%3Pd alloy: (a) a typical dislocation network in austenite phase, (b) bright-field electron micrograph of athermal plate martensite and selected area (indicated with a square) the electron diffaction pattern and corresponding key diagram, (c) bright and dark field electron micrograph of the martensite plate with twinning and the electron diffraction pattern of selected area.

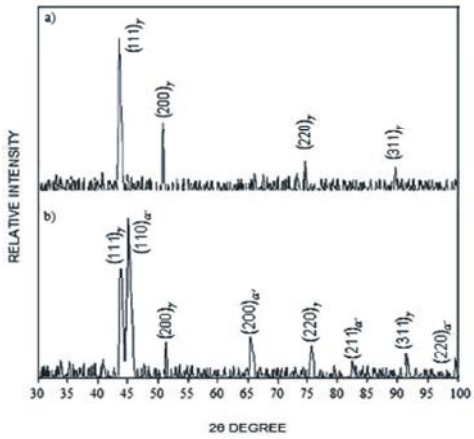

Fig. 4: X-Ray diffraction patterns for each speciemen of Fe-30%Ni-3%Pd alloy: (a) Speciemen of quenched in water at room temperature which homogenization at 1200°C for 6 h. (b) This speciemen after the 5 s liquid nitrogen (-196°C) immersion.

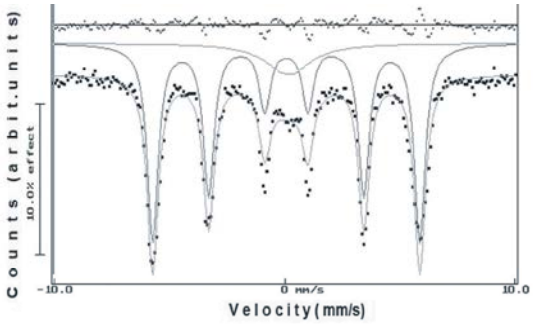

Fig. 5: Mössbauer spectra of Fe-30%Ni-3%Pd alloy, single peak represents the retained paramagnetic austenite phase and sextet represents the ferromagnetic (or antiferromagnetic) athermal martensite phase.

Moreover, Fig. 3c shows the other martensite plate formation with twinning. The crystallographic analysis revealed that the observed martensite twins are formed on the $\{112\}\alpha'\langle 111\rangle\alpha'$ system of the martensite and the

Table 2: Some Mössbauer parameters of studied Fe-30%Ni-3%Pd alloy

A (%)	M (%)	δ_A(mm/s)	δ_M(mm/s)	H (T)
23,59	76,41	0.133 0.003	0.431 0.021	34,983

observed existence of the dense twinnig on {112}α′ planes is consistent with the predictions of the crystallographic theories [29-33].

Crystal structures of alloy specimens were confirmed by an X-Ray diffraction measurement. Diffraction patterns of X-Ray were also given in Fig.4. As shown in the Fig. 4. X-Ray diffraction patterns which exhibit the fcc (γ) and bcc (α′) peaks. The mean value of the lattice parameter of the austenite and martensite phase calculated as 3.5704 ε and 2.8614 ε respectively. The results of X-Ray experiments agree that TEM and SEM observations.

Mössbauer spectra observed for the specimen of the examined alloy at room temperature is shown in Fig. 5. A typical six-line spectrum of the ferromagnetic (or antiferromagnetic) structure and also a singlet corresponding to the matrix austenite were observed after the heat treatments as reported earlier [15]. The Mössbauer parameters such as isomery shift and hyperfine magnetic field are given in Table 2 with the calculated volume fractions of the each phase. Previous Mössbauer studies have found that the hyperfine magnetic field is 32 T for Fe-%30 Ni alloy [16]. In this study, the internal magnetic field value of martensite was also calculated and found as 34,983 T in Fe-30%Ni-3%Pd alloy. Mössbauer study shows that the value of hyperfine magnetic field increases with an addition of Pd element.

CONCLUSIONS

The main findings in the present study would be summarized as follows:

- According to DSC results, the transformation kinetics found as athermal, namely martensitic phase transformation displayed the burst phenomenon in the studied alloy and M_s temperature don't display a major deviation with addition of 3%Pd to Fe-30%Ni binary alloy. On the other hand, compared with the other elements (Cr, Si, Mo), the element of Pd increases the M_s temperature.
- Mössbauer studies show that the value of hyperfine magnetic field increases with an addition of Pd element.
- From a morphologic viewpoint, thermally induced martensite exhibits plate morphology with twinnings in the Fe-30%Ni-3%Pd alloy and the crystallographic orientation relationship between the austenite and martensite exhibited a $(1\bar{1}0)_{\alpha'} // (\bar{1}11)_{\gamma}\ [111]_{\alpha'} // [110]_{\gamma}$ K-S type orientation relationship.
- The observed {112} α′ internal twins are of the proper variant to be the transformation twins of phenomenological theory.
- Observations of TEM shows two different martensite plate with twinning and untwined. The high dislocation density in untwined region of the plate martensite probably was blocking to twinning.
- X-Ray measurement on thermally induced martensite confirmed both SEM and TEM observation of α′ martensite formation and the mean value of the lattice parameter of the austenite and martensite phase calculated as 3.5704 ε and 2.8614 ε respectively.

REFERENCES

1. Nishiyama, Z., 1978. Martensitic Transformation, Academic Press, New York.
2. Kakeshita, T. and T. Fukuda, 2009. Effects of magnetic field on martensitic transformations, Journal of Physics, Conference Series, 165: 012-051.
3. Kakeshita, T., K. Shimizu, S. Funada and M. Date, 1985. Composition dependence of magnetic field-induced martensitic transformations in Fe-Ni Alloys, Acta Metall. 33, No.8, 1381.
4. Inokuti, Y. and B. Cantor, 1982. The microstructure and kinetics of martensite transformations, Acta Metall. 30, No.2, 1381.
5. Sridharan, K., F.J. Worzala and R.A. Dodd, 1991. Martensitic transformation and invar effect in Fe-Ni-Co alloys, Mater. Chem. and Phys., 30: 115.
6. Wayman, C.M. and K. Wakasa, 1981. Isothermal martensite formation in an Fe-20%Ni-5%Mn alloy, Metallography, 14: 37.
7. Durlu, T.N. and J.W. Christian, 1979. Effect of prior deformation on the martensite burst transformation in single crystals of an Fe-Ni-C alloy, Acta Metall., 27: 663.
8. Krauss, G. and A.R.Marder, 1971. The morphology of martensite in iron alloys, Metall. and Mater. Trans. B., 2: 2343.
9. Seo, S., D. S. Leem, J. H. Jun and C.S. Chai, 2001. Effect of thermal cycling on microstructures and mechanical properties of lath and lenticular martensites in Fe-Ni alloys, ISIJ Int., 41: 350.

10. Umemoto, M., E. Yoshitake and I. Tamura, 1983. The morphology of martensite in Fe-C, Fe-Ni-C and Fe-Cr-C alloys, J. Mater. Sci., 18: 2893.
11. Kirindi, T. and M. Dikici, 2006. Microstructural analysis of thermally induced and deformation induced martensitic transformations in Fe-12.5 wt.% Mn-5.5 wt. % Si-9wt. % Cr-3.5wt. % Ni alloy, J. Alloys Compd., 407: 157.
12. Visvesvaran, P., 1996. A study on morphology and plate mean dimensions in Fe-Ni and Fe-Ni-Cr alloys, Metall. and Mater. Trans. A, 27: 973.
13. Kajiwara, S., 1981. Morphology and crystallography of the isothermal martensite transformation in Fe-Ni-Mn alloys, Philos. Mag. A, 43: 1483.
14. Bunshah, R.F. and R.F. Mehl, 1953. Rate of propagation of martensite, Journal of Metals, 5: 1251.
15. Yasar, E., H. Gungunes, A. Kilic and T.N. Durlu, 2006. Effect of Mo on the magnetic properties of martensitic phase in Fe-Ni-Mo alloys, J. Alloys Compd., 424: 51.
16. Binnatov, K.G. and A.O. Mekhrabov, 2001. Mössbauer Effect Study of Fine Atomic Structure of Fe-Ni-C Alloys, Turk. J. Phy., 25: 121.
17. Novak, P. and V. Chian, 2010. Contact hyperfine field at Fe nuclei from density functional calculations, Physical Review B, 81: 174412.
18. Birsan, M., B. Fultz and L.Anthony, 1997. Magnetic properties of bcc Fe-Pd extended solid solutions, Physical Review B, 55: 502.
19. Troiano, A.R. and A.B. Greninger, 1946. The martensite transformation, Metal Progress, 50: 303.
20. Christian, J.W., 1979. ICOMAT, Cambridge, Massachusetts, USA,
21. Ya, I. Georgiva and I.I. Nikitina, 2004. Isothermal and athermal martensitic transformations, Metal Science and Heat Treatment, 14(5): 452.
22. Kaufman, L. and M. Cohen, 1956. The martensitic transformation in the Iron-Nickel system. Trans. AIME, J. Metals, 206: 1393.
23. Kitihara, H., R. Ueji, M. Ueda, N. Tsuji and Y. Minamino, 2005. Crystallographic analysis of plate martensite in Fe-28.5 at%Ni by FE-SEM/EBSD, Mater. Charac., 54: 378.
24. Shibata, A., S. Morito, T. Furuhara and T. Maki, 2009. Substructures of lenticular martensites with different martensite start temperatures in ferrous alloys, Acta Materialia, 57: 483.
25. Himuro, Y., R. Kainuma and K. Ishida, 2002. Martensitic Transformation and Shape Memory Effect in Ausaged Fe-Ni-Si Alloys, ISIJ Int., 42: 184.
26. Olson, G.B. and M. Cohen, 1976. A general mechanism of martensitic nucleation: Part I. General concepts and the FCC?HCP transformation, Metall. Trans. A, 7: 1897.
27. Yasar, E., H. Gungunes, S. Akturk and T.N. Durlu, 2007. New observations on the formation of athermal martensite in Fe-Ni-Mo alloys, J. Alloys Compd., 428: 125.
28. Yang, J.H. and C.M. Wayman, 1992. Self-accomodation and shape memory mechanism of ε- martensite-I.Experimental observations, Mater. Charact. 28: 23.
29. Wechsler, M.S., D.S. Lieberman and T.A. Read, 1953. On the theory of the formation of martensite, Trans. AIME, Journal of Metals, 197: 1503.
30. Bowles, J.S. and J.K. Mackenzie, 1954. The crystallography of martensite transformations I, Acta Metallurgica, 2: 129.
31. Mackenzie, J.K. and J.S. Bowles, 1954. The crystallography of martensite transformations II, Acta Metallurgica, 2: 138.
32. Bowles, J.S. and J.K. Mackenzie, 1954. The crystallography of martensite transformations III. Face-centred cubic to body-centred tetragonal transformations, Acta Metallurgica, 2: 224.
33. Mackenzie, J.K. and J.S. Bowles, 1957. The crystallography of martensite transformations IV. Body-centred cubic to orthorhombic transformations, Acta Metallurgica, 5: 137.